Electronic Supporting Information

3D Carbon Foam Supported WS_2 Nanosheets for Cable-shaped Flexible Sodium Ion Batteries

Ye Wang,[a,b] Dezhi Kong,[b] Shaozhuan Huang,[b] Yumeng Shi,[b,c] Meng Ding,[b] Yew Von Lim,[b] Tingting Xu,[a] Fuming Chen,[c] Xinjian Li,[a] and Hui Ying Yang[c,*]

[a] Key Laboratory of Materials Physics of Ministry of Education, Department of Physics and Engineering, Zhengzhou University, Zhengzhou 450052, China

[b] Pillar of Engineering Product Development, Singapore University of Technology and Design, 8 Somapah Road, 487372, Singapore

[c] SZU-NUS Collaborative Innovation Center for Optoelectronic Science & Technology, Key Laboratory of Optoelectronic Devices and Systems of Ministry of Education and Guangdong Province, College of Optoelectronic Engineering, Shenzhen University, Shenzhen 518060, China

*Corresponding author. Tel.: +65 6303 6663; Fax: +65 6779 5161. E-mail address: yanghuiying@sutd.edu.sg (H. Y. Yang)

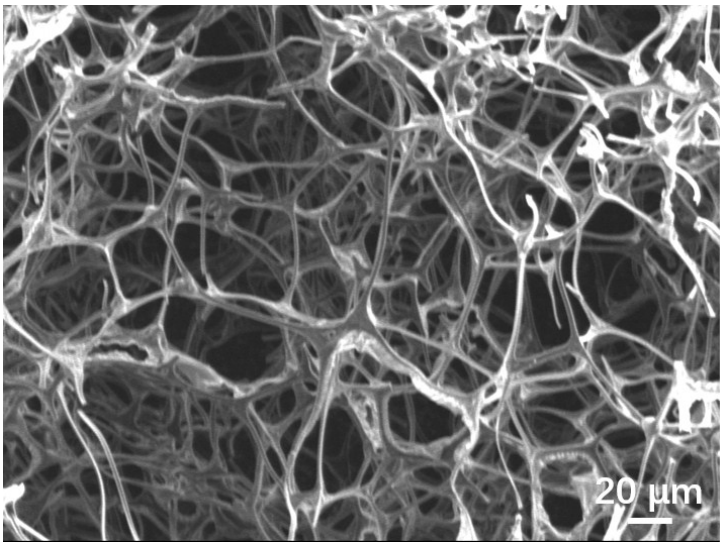

Fig. S1. SEM image of the carbonized melamine foam.

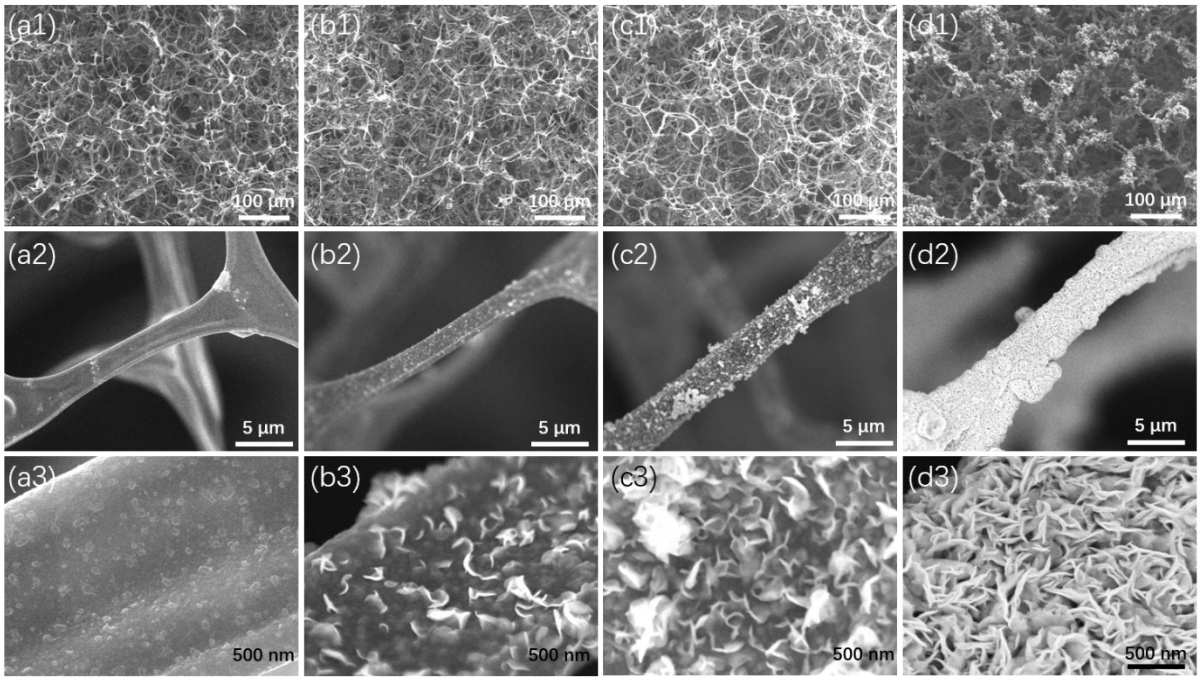

Fig. S2. SEM images of WS_2/3DCF with various solvothermal reaction times: (a) 1 hour, (b) 3 hours, (c) 6 hours and (d) 12 hours.

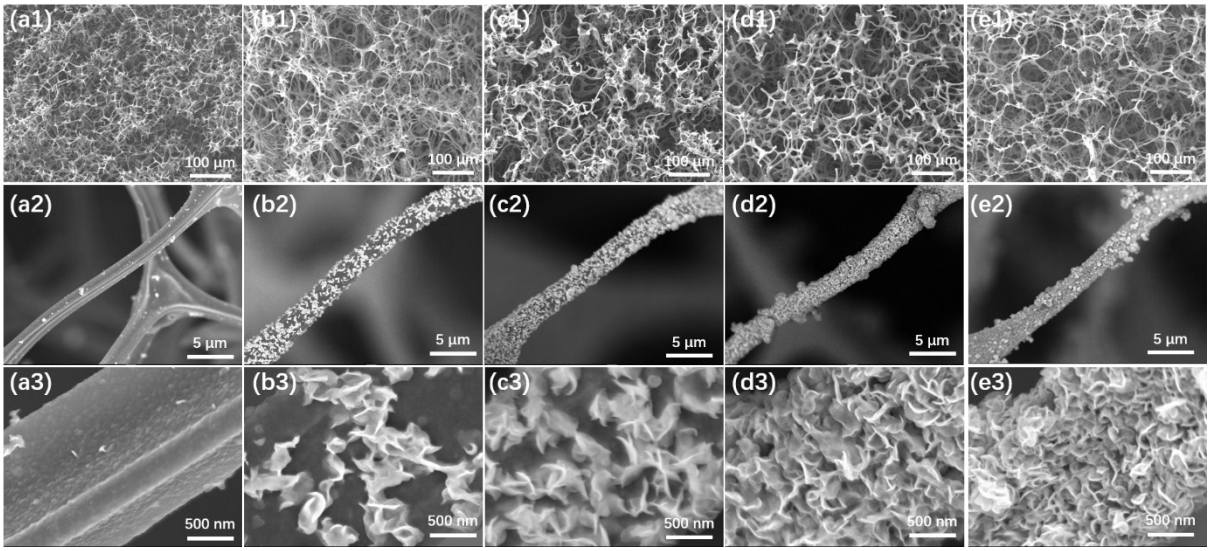

Fig. S3. SEM images of WS_2/3DCF with various plasma treatment durations: (a) 0 s, (b) 10 s, (c) 30 s, (d) 120 s and (e) 600 s.

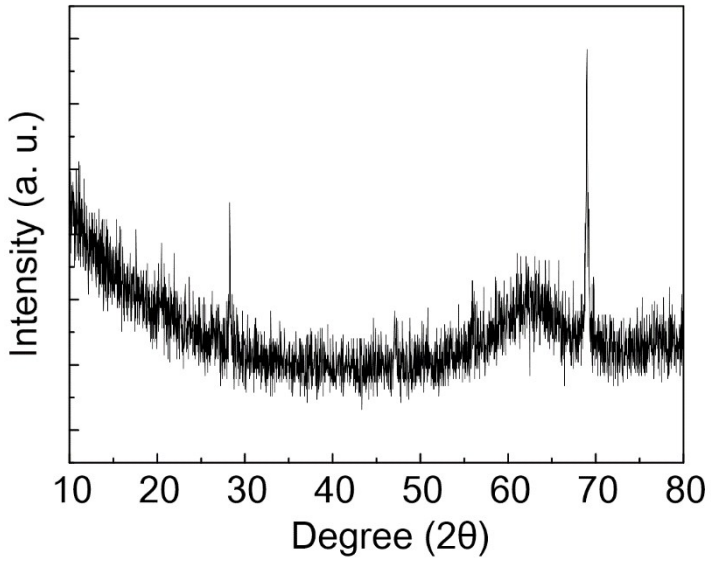

Fig. S4. XRD pattern of the silicon holder background.

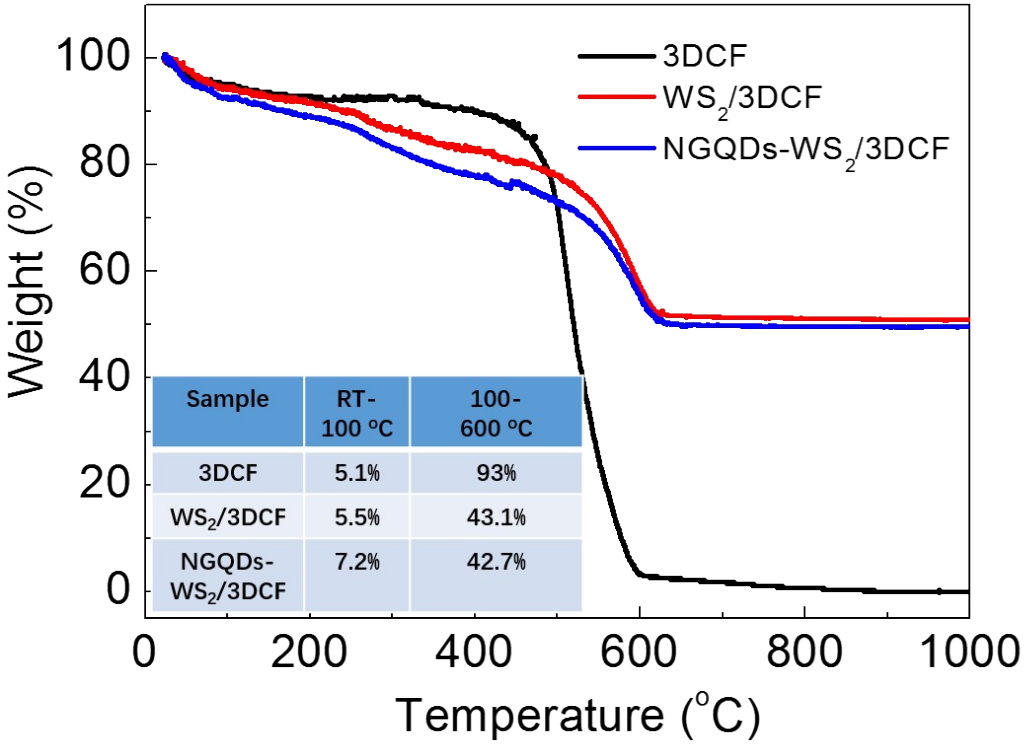

Fig. S5. TGA curves of 3DCF, WS_2/3DCF and NGQDs-WS_2/3DCF nanocomposites. Insert: weight loss during the temperature range of RT - 100 °C and 100 – 600 °C.

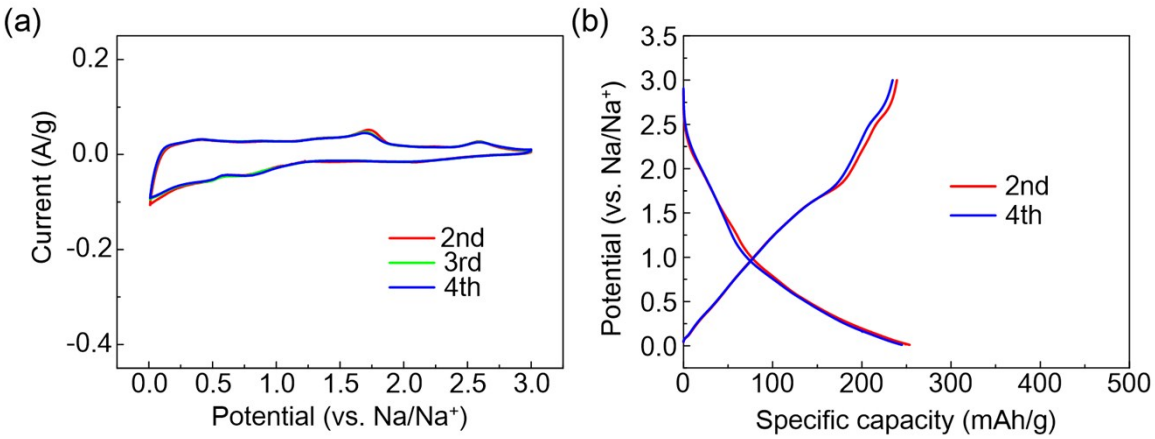

Fig. S6. (a) CV curve of the WS_2/3DCF electrode of the 2nd to 4th cycles at a scan rate of 0.1 mV s^{-1} in a potential range of 0.01–3.00 V vs. Na/Na^+. (b) Galvanostatic discharging/charging curves of the WS_2/3DCF electrode at a current density of 50 mA g^{-1} for the 2nd and 4th cycles.

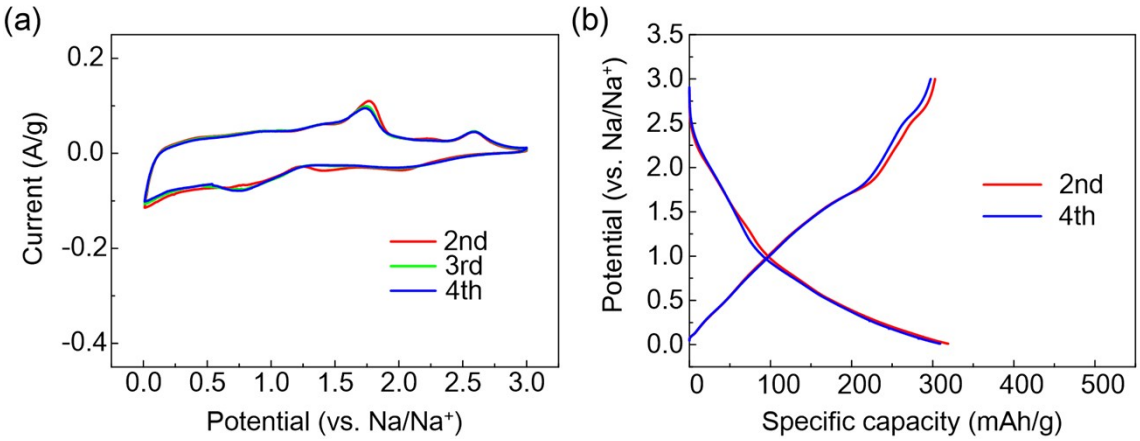

Fig. S7. (a) CV curve of the NGQDs-WS_2/3DCF electrode of the 2nd to 4th cycles at a scan rate of 0.1 mV s^{-1} in a potential range of 0.01–3.00 V vs. Na/Na^+. (b) Galvanostatic discharging/charging curves of the WS_2-NGQDs/3DCF electrode at a current density of 50 mA g^{-1} for the 2nd and 4th cycles.

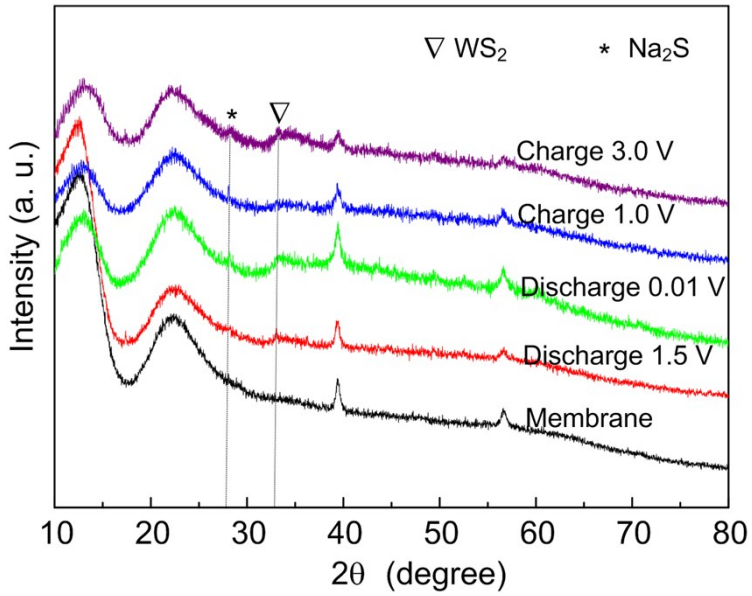

Fig. S8. Ex-situ XRD patterns of WS_2/3DCF electrodes at various discharge/charge voltages. Before ex-situ XRD measurement, WS_2/3DCF electrode with membrane was disassembled in a glove box when discharged/charged to a fixed voltage, and sealed in a kapton tape.

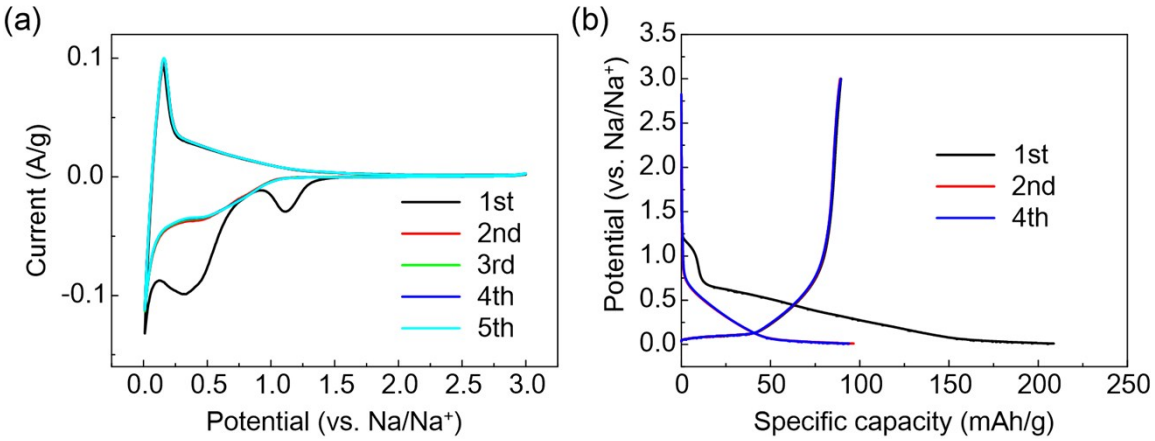

Fig. S9. (a) CV curve of the 3DCF electrode of the 2nd to 4th cycles at a scan rate of 0.1 mV s^{-1} in a potential range of 0.01–3 V vs. Na/Na^+. (b) Galvanostatic discharging/charging curves of the 3DCF electrode at a current density of 50 mA g^{-1} for the 1st, 2nd and 4th cycles.

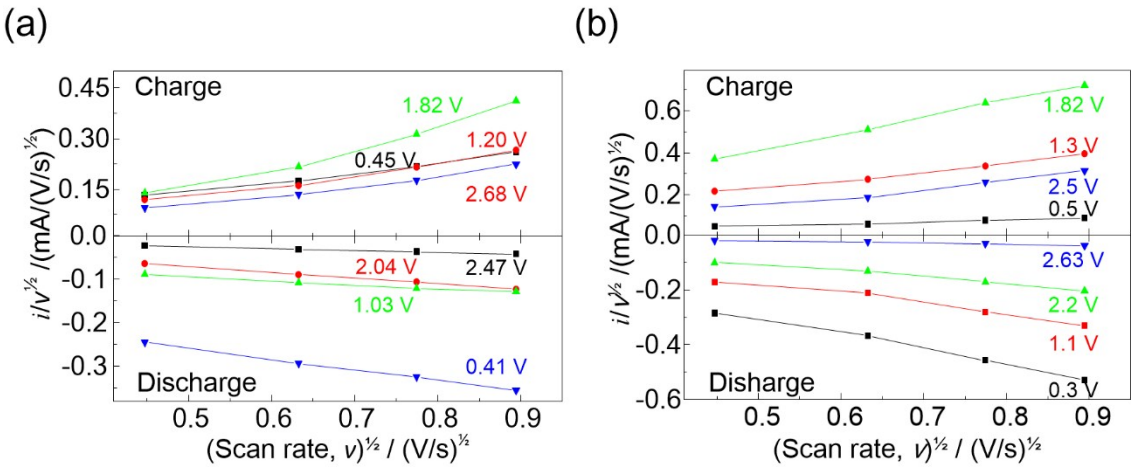

Fig. S10. (a) and (b) plot of $v^{1/2}$ vs. $i(V)/v^{1/2}$ to calculate the constants of k_1 and k_2 of WS_2/3DCF and NGQDs-WS_2/3DCF electrodes, respectively.

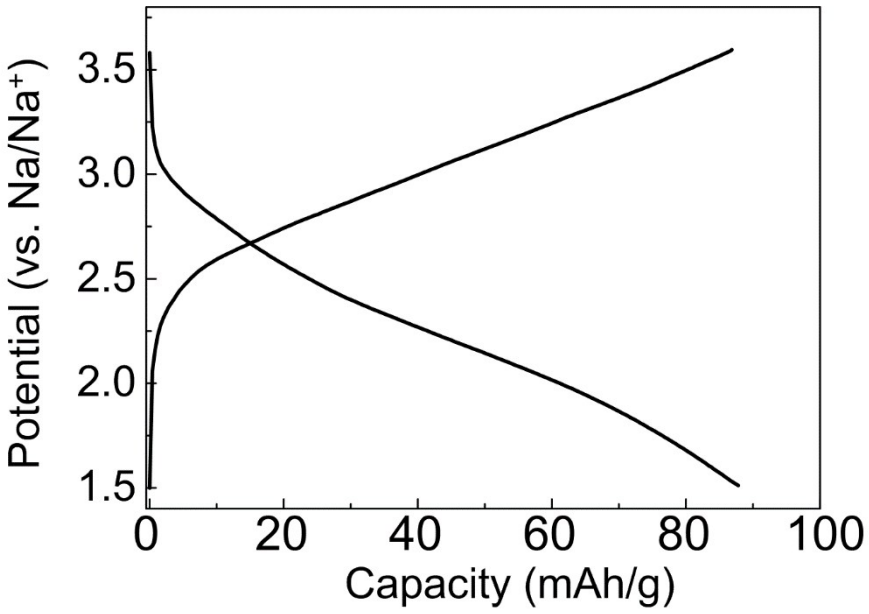

Fig. S11. Galvanostatic charge and discharge curves of the 3rd cycle of $Na_{0.44}MnO_2$ cathode at a current density of 50 mA g^{-1}.

Table S1. Fitting results of the EIS curves in Fig. 5d using the equivalent circuit model

Sample	R_s (Ω)	R_f (Ω)	R_{ct} (Ω)
3DCF	3.429	216.6	105.1
WS_2/3DCF	4.873	238.1	376.8
NGQDs-WS_2/3DCF	4.039	227.5	237

Table S2. Comparison of the electrochemical performance and synthesis method of the WS_2 based anode materials of SIBs.

Composites	**Synthesis method**	**Cycling stability (mAh g^{-1}/cycles/mA g^{-1})**	**Rate capability (mAh g^{-1}/mA g^{-1})**	**Ref**
NGQDs-WS_2/3DCF	Solvothermal + 500 ^oC annealing	392.1/1000/200	460.9/50, 436.4/100, 417.1/200, 357.4/500, 312.2/1000, 268.4/2000, 211.4/5000	This work
WS_2/CNT-rGO ordered 3D aerogel	Solvothermal + 500 ^oC annealing+freeze drying	252.9/100/200	311.4/100, 302.8/200, 289/500, 262.8/1000, 221.1/2000, 129.2/5000, 47.2/10000	[1]
WS_2 nanosheets/N-doped carbon	Chemical vapor deposition	~200/100/100	349/100, 313/300, 282/500, 258/1000	[2]
WS2@NC	Solvothermal + 500 ^oC annealing	70/500/5000	384/100, 360/200, 336/500, 302/1000, 236/2000, 151/5000	3
WS_2/C	Electrostatic spray deposition+450 ^oC Ar/H_2 + 600 ^oC Ar	219/300/500	393/100, 270/500, 199/1000, 81/5000	[4]
WS_2@graphene	Hydrothermal	329/500/20, 283/500/40, 218/500/80, 170/500/160, 148/500/320, 94/500/640	329/20, 283/40, 218/80, 170/160, 148/320, 94/640	[5]
WS_2-3D RGO	Spray pyrolysis + sulfidation	334/200/200	404/100, 287/900	[6]

References

1. Y. Wang, D. Kong, W. Shi, B. Liu, G. J. Sim, Q. Ge and H. Y. Yang, *Adv. Energy Mater.*, 2016, **6**, 1601057.

2. X. Wang, J. F. Huang, J. Y. Li, L. Y. Cao, W. Hao and Z. W. Xu, *ACS Appl. Mater. Interfaces*, 2016, **8**, 23899-23908.

3. Y. Von Lim, Y. Wang, L. Guo, D. Kong, R. Ang, H. Y. Yang, *J. Mater. Chem. A.* **2017**, *5*, 10406-10415.

4. C. Zhu, P. Kopold, W. Li, P. A. van Aken, J. Maier and Y. Yu, *J. Mater. Chem. A.*, 2015, **3**, 20487-20493.

5. D. Su, S. Dou and G. Wang, *Chem. Commun.*, 2014, **50**, 4192-4195.

6. S. H. Choi and Y. C. Kang, *Nanoscale*, 2015, **7**, 3965-3970.